Electronic Supporting Information

Surface-enhanced Raman spectroscopy for simultaneously sensitive detection of multiple microRNAs in lung cancer cells

Li-Ping Ye,[‡a] Juan Hu,[‡a] Li Liang[‡b] and Chun-yang Zhang*[a]

[a] Single-Molecule Detection and Imaging Laboratory, Shenzhen Institutes of Advanced Technology, Chinese Academy of Sciences, Guangdong 518055, China

[b] Department of Tumor Chemotherapy and Radiation Sickness, Peking University Third Hospital, Beijing 100191, China

[‡] These authors contributed equally

* To whom correspondence should be addressed. E-mail: zhangcy@siat.ac.cn

EXPERIMENTAL SECTION

Materials. The HPLC-purified microRNAs and PAGE-purified DNA oligonucleotides (Table S1) were synthesized by TaKaRa Biotechnology Co., Ltd. (Dalian, China). The deoxynucleotide solution mixture (dNTPs), RNase inhibitor and diethyl pyrocarbonate (DEPC)-treated water were obtained from TaKaRa Bio. Inc. (Dalian, China). The Vent (exo-) DNA polymerase and nicking endonuclease Nt.BstNBI were purchased from New England Biolabs (Ipswich, MA, USA). All other reagents were purchased from China National Medicines Co. Ltd. (Beijing, China).

Table S1. Sequences of the oligonucleotides [a]

note	sequence (5'-3')
miR-205	UCC UUC AUU CCA CCG GAG UCU G
one-base mismatched miRNA	UCC UUC AUU C<u>U</u>A CCG GAG UCU G
miR-7157	<u>UCA</u> G<u>C</u>A UUC AUU G<u>G</u>C ACC <u>A</u>GA G<u>A</u>
miR-126	UCG UAC CGU GAG UAA UAA UGC G
trigger-205	CAT CCT AGC AGT CAG TGA GCA TC
template-205	GAT GCT CAC TGA CTG CTA GGA TGG TAT GAC TCG ATG CTC ACT GAC TGC TAG GAT GGT ATG ACT CCA GAC TCC GGT GGA ATG AAG GA
template-126	ATG GTA TCT GCA CTG CTA GGA TGG TAT GAC TCA TGG TAT CTG CAC TGC TAG GAT GGT ATG ACT CCG CAT TAT TAC TCA CGG TAC GA
capture probe	CTG CTA GGA TG TTT TTT TTT - SH
reporter probe-205	TAMRA - GAT GCT CAC TGA
reporter probe-126	Cy3 - ATG GTA TCT GCA

[a] The underlined bases in the one-base mismatched miRNA and miR-7157 symbolize the bases different from those of miR-205 sequences.

EXPAR Reaction. The reaction mixtures for EXPAR were prepared separately on ice as part I and part II. Part I consisted of 150 nM template, 250 μM dNTPs, 0.8 U/μL RNase inhibitor, 0.5× Nt.BstNBI buffer (25 mM Tris-HCl, pH 7.9, 50 mM NaCl, 5 mM $MgCl_2$, 0.5 mM dithiothreitol),

and the miRNA target. Part II consisted of 0.5 U/μL nicking endonuclease Nt.BstNBI, 0.06 U/μL Vent (exo-) DNA polymerase, 1× ThermoPol buffer (20 mM Tris-HCl, pH 8.8, 10 mM KCl, 10 mM $(NH_4)_2SO_4$, 2 mM $MgSO_4$, 0.1% Triton X-100), and DEPC-treated water. These two parts were mixed immediately before being transferred to the PCR system. The EXPAR reaction was performed in a volume of 10 μL at 55 °C for 20 min.

EXPAR was monitored in real time at intervals of 30 s with 1× SYBR Green I (Invitrogen, USA) as the fluorescent indicator in a BIO-RAD CFX connect™ Real-Time system (Singapore). The products of amplified reaction were also analyzed by 12% nondenaturating polyacrylamide gel electrophoresis (PAGE) in 1× TBE buffer (9 mM Tris-HCl, pH 7.9, 9 mM boric acid, 0.2 mM EDTA) at a 110 V constant voltage for 40 min at room temperature. The gel was stained by 5× SYBR Green I and scanned by a Kodak Image Station 4000MM (Rochester, NY, USA). The band intensities in the gels were analyzed by Quantity One software.

Preparation of Capture Probe-Modified AuNPs. The capture probe-modified Au nanoparticals (AuNPs) was prepared according to the reported protocols with a slight modification.[1] The AuNPs with a center diameter of 56 nm shows a UV-vis absorption peak at 535 nm (Figure S3).[2] Thiol-modified DNA was functionalized onto the nanoparticles as follows. The 3′-thiol modified capture probes (5.6 nmol) were added to 2 mL of AuNP solution (1.34 nM), and then the solution was aged overnight at 4 °C. Phosphate buffer (pH 7.0) and NaCl were added dropwisely to obtain a solution containing 10.0 mM phosphate buffer and 0.1 M NaCl, followed by centrifugation to remove the excess oligonucleotides. After the supernatant was removed, the soft pellet in the bottom was washed with phosphate buffer and resuspended in 0.3 M PBS (10.0 mM phosphate

buffer and 0.3 M NaCl). In the capture probe-modified AuNP solution, the AuNPs was estimated to be 2.68 nM, and the DNA concentration was estimated to be 2.05 μM according to the previous report.[3]

SERS Assay. The 100 μL of capture probe-modified AuNP solution was mixed with 10 μL of reporter probe (10 μM) and 10 μL of amplification products. The mixture was incubated at 75 °C for 3 min, followed by slowly cooling to room temperature. After the centrifugation, the solution was rinsed for three times with 0.3 M PBS containing 0.01% tween-20. Finally, the 2 μL of soft pellet in the bottom was dropped onto a cleaned Si surface and dried in air slowly. The SERS spectra were measured by a LabRAM HR Raman Spectrometer (HORIBA Jobin-Yvon, France) with a laser at the excitation wavelength of 632.8 nm and 15.7 mW power irradiation. The collection time for each spectrum was 10 s. The average spectra were obtained from five random spots to make sure the uniformity of the signal. The AFM image shows the relatively uniformed surface morphology in the 30 μm × 30 μm area (Figure S4A), and the typical aggregates cover an area of ~3 μm^2 with a height of ~400 nm (Figure S4B). The uniformity of SERS signals is confirmed by the signals collected from 20 random spots (Figure S4C) with relative standard deviations (RSD) of 6.8% (Figure S4D). These results reveal that the obtaining SERS signals exhibit excellent reproducibility.[4,5] In addition, the SERS signal varies with the concentration of target miRNA, and we can quantitatively analyze the concentration of target miRNA by measuring the Raman intensity (Fig. 1B). The obtained results show statistically significance for different concentrations of target miRNA (unpaired t test, $P < 0.05$).

MicroRNAs Extraction and Quantitative Polymerase Chain Rreaction. The human bronchial epithelial cell line Beas-2B and NSCLC cell lines A549, NCI-H596 (H596) and SK-MES-1 were kindly supplied by Shenzhen University (Shenzhen, China) and cultured in RPMI 1640 medium supplemented with 10% fetal bovine serum (Invitrogen, USA) in a humidified incubator containing 5% CO_2 at 37 °C. The total RNA, including miRNA, was extracted from ~10^7 cells using an RNeasy Mini Kit (Qiagen, Valencia, CA, USA). The total RNA including miRNA was extracted from the clinical tissues using miRNeasy FFPE kit (Qiagen, Germany) according to the manufacturer's procedure. The concentrations of RNAs were measured by a spectrophotometer at the absorbance of 260 nm. Quantitative polymerase chain reaction (qPCR) was employed for the quantification of miRNA (Figure S6) using NCode™ EXPRESS SYBR® GreenER™ miRNA qRT-PCR Kit (Invitrogen, USA) in a BIO-RAD CFX connect™ Real-Time system (Singapore).

Supplementary results

The target miRNA-induced EXPAR reaction is confirmed by real time fluorescence measurement as well as PAGE analysis (Fig. S1). In the presence of target miR-205, the fluorescence intensity increases in a sigmoidal fashion and reaches a plateau within 15 min (Fig. S1A, red line), suggesting that miR-205 initiates the EXPAR reaction. While in the absence of miR-205, the fluorescence intensity remains unchanged until 20 min (Fig. S1A, black line). It should be noted that the control reaction without miR-205 shows nonspecific background amplification over 20 min, but it does not affect the subsequent analysis due to the fixed reaction time of 20 min for EXPAR in this research. The distinct band of trigger (23 nt) is observed in the presence of miR-205 (Fig. S1B, lane 3), but no such a band is observed in the control group without miR-205

(Fig. S1B, lane 2). In the absence of either template or polymerase, neither significant fluorescence signal (Fig. S1A, blue line and green line) nor distinct band of trigger (Fig. S1B, lanes 4 and 5) is observed. In the absence of nicking enzyme, the polymerase can bind to a template and synthesize the DNA complementary to the template in an unprimed fashion,[6] resulting in the generation of a fluorescence signal (Fig. S1A, purple line), but no band of trigger is observed in PAGE analysis (Fig. S1B, lane 6) because the replicated DNA strand cannot be cleaved by Nt.BstNBI. As shown in Fig. S1C, in the presence of miR-205, template, polymerase and nicking enzyme, strong characteristic SERS signal is observed (Fig. S1C, red line). The characteristic peaks at 1219, 1356, 1509, 1536, and 1651 cm^{-1} are consistent with the previously reported TAMRA-labeled SERS signal.[7] The non-overlapping and strongest Raman band at 1651 cm^{-1} is selected as the signal for TAMRA-labeled reporter probe in the subsequent analysis. In contrast, no significant SERS signal is observed in the absence of miR-205 despite of some weak SERS signal due to the nonspecific adsorption of the reporter probes on the surface of the AuNPs.[1,5] These results demonstrate that the EXPAR-based SERS can be applied for sensitive detection of miR-205.

Optimization of EXPAR Reaction. The amplification efficiency of EXPAR is very crucially affected by Vent (exo-) DNA polymerase and Nt.BstNBI nickase.[8] We first employed real-time fluorescence measurement to investigate the influence of Vent (exo-) DNA polymerase upon the amplification efficiency in the presence of 10 nM miR-205 at a fixed concentration of Nt.BstNBI (0.4 U/μL). The blank is the negative control without target miR-205, and the ΔPOI of fluorescence curves is used for quantitative evaluation (the POI is defined as the time

corresponding to the maximum slope in the fluorescence curve, and the ΔPOI is defined as the difference in the POI value between a miRNA sample and the blank). As shown in Figure S2A, the ΔPOI reaches the maximum at 0.06 U/μL Vent (exo-) DNA polymerase. Thus, 0.06 U/μL Vent (exo-) DNA polymerase is selected in the subsequent research. Figure S2B shows the variance of ΔPOI with the concentration of Nt.BstNBI at a fixed concentration of Vent (exo-) DNA polymerase (0.06 U/μL). In the presence of miR-205, the ΔPOI increases with the increasing concentration of Nt.BstNBI from 0.2 U/μL to 0.5 U/μL, but tends to level off beyond the concentration of 0.5 U/μL. Thus, 0.5 U/μL Nt.BstNBI is selected in the subsequent research.

The amplification efficiency of EXPAR is crucially affected by the template as well.[8] As shown in Figures S2C and S2D, the band intensity of trigger (i.e. the amplification products) increases with the increasing concentration of template from 50 nM to 150 nM, followed by the decrease beyond the concentration of 150 nM. This result can be explained by following two factors: (1) low template concentration might be unable to hybridize with the available miRNAs; (2) Even though high template concentration might result in high hybridization efficiency and generation of abundant products, the released triggers can further hybridize with the excess templates as well. Both factors can adversely affect the amplification efficiency of EXPAR. Consequently, 150 nM template is selected in the subsequent research.

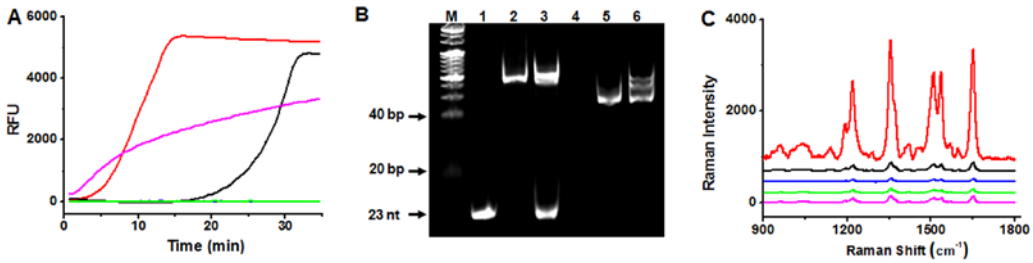

Figure S1. (A) Real-time fluorescence measurement of EXPAR reaction triggered by miR-205. The fluorescence curves are obtained in the presence (red line) and in the absence of miR-205 (black line), in the presence of miR-205 but without the template (blue line), without Vent (exo-) DNA polymerase (green line), without Nt.BstNBI (purple line), respectively. RFU represents the relative fluorescence units. (B) PAGE analysis of EXPAR products. Lane M is the DNA ladder marker; lane 1 is the synthesized trigger (23 nt); lanes 2-6 represent the amplification products in the absence of miR-205 (line 2), in the presence of miR-205 (line 3), in the absence of template (line 4), in the absence of Vent (exo-) DNA polymerase (line 5), in the absence of Nt.BstNBI (line 6). (C) SERS spectra obtained in the presence (red line) and in the absence of miR-205 (black line), in the presence of miR-205 but without the template (blue line), without Vent (exo-) DNA polymerase (green line), without Nt.BstNBI (purple line), respectively. The concentration of miR-205 is 10 nM, and the concentration of template is 150 nM.

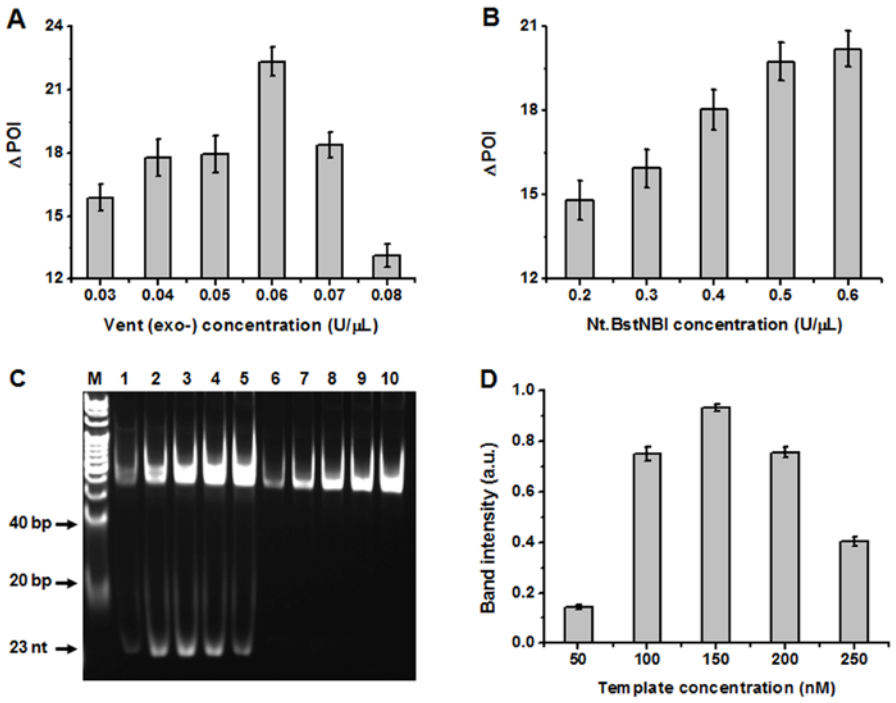

Figure S2. Optimization of EXPAR reaction. (A) Influence of the concentration of Vent (exo-) DNA polymerase upon the amplification efficiency at a fixed concentration of Nt.BstNBI (0.4 U/μL). (B) Influence of the concentration of Nt.BstNBI upon the amplification efficiency at a fixed concentration of Vent (exo-) DNA polymerase (0.06 U/μL). The concentration of template is 100 nM. (C) Influence of the template concentration upon the amplification efficiency in the presence of miR-205 (lanes 1, 2, 3, 4 and 5) and in the absence of miR-205 (lanes 6, 7, 8, 9 and 10) at the concentration of Vent (exo-) DNA polymerase (0.06 U/μL) and Nt.BstNBI (0.5 U/μL). Lane M is 20-bp DNA ladder marker. Lanes 1 and 6, the concentration of template is 50 nM; lanes 2 and 7, the concentration of template is 100 nM; lanes 3 and 8, the concentration of template is 150 nM; lanes 4 and 9, the concentration of template is 200 nM; lanes 5 and 10, the concentration of template is 250 nM. (D) Quantitative analysis of the effect of template concentration on the amplification efficiency. The band intensity is quantified using Quantity One software. The concentration of miRNA-205 is 10 nM. Error bars show the standard deviation of three experiments.

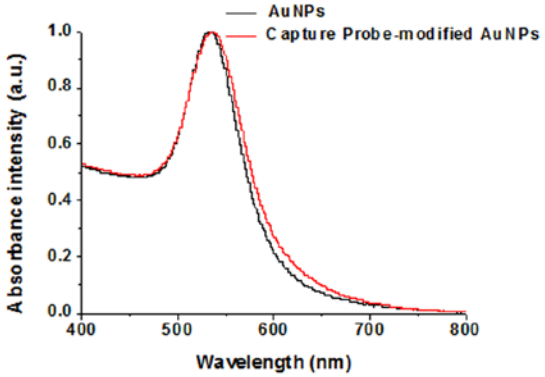

Figure S3. Normalized UV-vis absorption spectra of AuNPs (black line) and capture probe modified-AuNPs (red line).

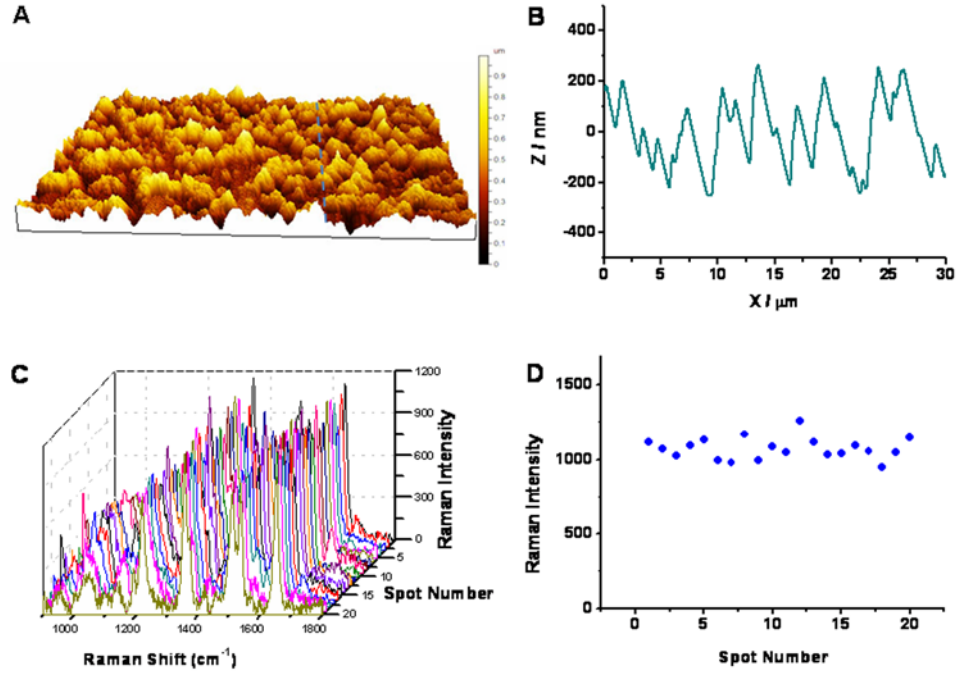

Figure S4. (A and B) The 3D image (A) and the height (B) of the sample on Si surface with an area of 30 μm × 30 μm measured by AFM. (C and D) SERS spectra (C) and the Raman intensity (D) at 1651 cm^{-1} obtained from 20 random spots. The concentration of miRNA-205 is 1 pM.

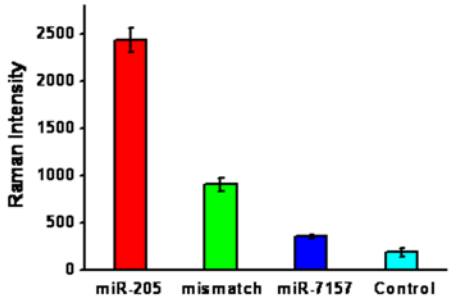

Figure S5. Raman intensity at 1651 cm^{-1} in response to 10 nM miR-205 (red column), 10 nM one-base mismatched miRNA (green column), 10 nM miR-7157 (blue column), and the control group without any miRNAs (cyan column). Error bars show the standard deviation of three experiments.

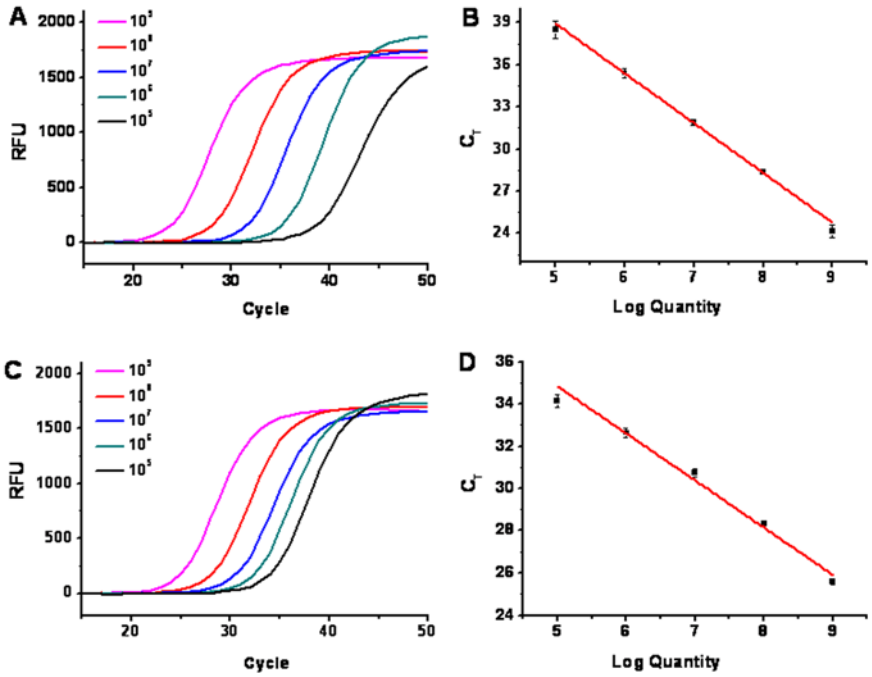

Figure S6. (A) Quantitative real-time fluorescence monitoring of the qPCR reactions triggered by miR-126 at different quantity. RFU represents the relative fluorescence units. (B) The threshold cycle (C_T) value obtained from the data (A) as a function of the logarithmic starting quantity of miR-126. (C) Quantitative real-time fluorescence monitoring of the qPCR reactions triggered by miR-205 at different quantity. (D) C_T value obtained from data (C) as a function of the logarithmic starting quantity of miR-205. Error bars show the standard deviation of three experiments.

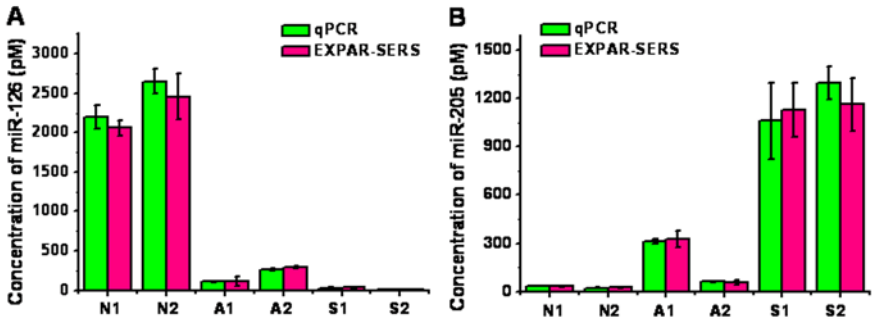

Figure S7. Concentrations of miR-126 (A) and miR-205 (B) in lung tissue samples measured by qPCR (green column) and EXPAR-based SERS (purple column). N1, N2, A1, A2, S1, S2, represent Normal 1, Normal 2, Adenocarcinoma 1, Adenocarcinoma 2, Squamous cell lung carcinoma 1, Squamous cell lung carcinoma 2, respectively. The 1 μL of extracted total RNA sample (100 ng) was added to each reaction system for measurement. Error bars show the standard deviation of three experiments.

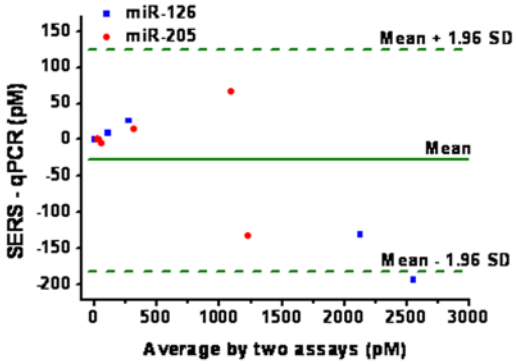

Figure S8. Result of the Bland-Altman analysis between EXPAR-SERS and qPCR.

Table S2. Recovery results of miR-205 spiked in normal lung tissue samples (N1) and squamous cell lung carcinoma tissue samples (S1).

Sample	Detected (pM)	Added (pM)	Found (pM)	Recovery rate (%)
N1	32.96	100	124.85 ± 5.62	94.31
S1	1126.94	1000	1942.09 ± 99.54	90.52

References

1. J. Hu and C. Y. Zhang, *Anal. Chem.*, 2010, **82**, 8991.
2. K. R. Brown, D. G. Walter and M. J. Natan, *Chem. Mater.*, 2000, **12**, 306.
3. S. J. Hurst, A. K. Lytton-Jean and C. A. Mirkin, *Anal. Chem.*, 2006, **78**, 8313.
4. J. Hu, B. Zhao, W. Xu, Y. Fan, B. Li and Y. Ozaki, *Langmuir*, 2002, **18**, 6839.
5. G. Wang, R. J. Lipert, M. Jain, S. Kaur, S. Chakraboty, M. P. Torres, S. K. Batra, R. E. Brand and M. D. Porter, *Anal. Chem.*, 2011, **83**, 2554.
6. E. Tan, B. Erwin, S. Dames, T. Ferguson, M. Buechel, B. Irvine, K. Voelkerding and A. Niemz, *Biochemistry*, 2008, **47**, 9987.
7. Y. C. Cao, R. Jin and C. A. Mirkin, *Science*, 2002, **297**, 1536.
8. J. Van Ness, L. K. Van Ness and D. J. Galas, *P. Natl Acad. Sci. USA*, 2003, **100**, 4504.